Suspecting Less and Doing Better: New Insights on Palmprint Identification for Faster and More Accurate Matching

Qian Zheng, Ajay Kumar, and Gang Pan

***Abstract*— This paper introduces a generalized palmprint identification framework to unify several state-of-art 2D and 3D palmprint methods. Through this framework, we argue that the methods employing one-to-one matching strategy and binary representation for feature are more effective for palmprint identification. The analysis for the first argument is based on a statistical matching model and is supported by outperforming results on several publicly available 2D palmprint databases. These two arguments are further evaluated for 3D palmprint matching and used to introduce a new method for encoding 3D palmprint feature. The proposed 3D feature is binary and more efficiently computed. It encodes the 3D shape of palmprint to either convex or concave. The experimental results on two publicly available, from contactless and contact-base 3D palmprint database of 177 and 200 subjects, respectively, outperform the state-of-the-art methods. This paper also provides our palmprint matching algorithm(s) in public domain, unlike the previous work in this area, which will help to further advance research efforts in this area.**

***Index Terms*— 3D palmprint, 2D palmprint, contactless palmprint matching.**

I. Introduction

AUTOMATED personal identification using biometrics characteristics is one of the most critical and challenging tasks to meet growing demand for stringent security. There is ever growing need to develop more accurate and efficient biometrics matching technologies, especially for applications like those in national ID programs such as UIDAI [21] and HANIS [24]. Therefore our objective in this paper has been to design, develop and evaluate more accurate, compact and faster matching algorithms for the palmprint identification. In the context of advancements in the matching of matching 2D and 3D palmprints, this work introduces new algorithms to further advance feature extraction and matching techniques in this area.

Automated personal identification using palmprint images has attracted a lot of attention from the researchers and several methods [1], [2], [7], [8], [14]–[16] have been proposed in the literature. Reference [27] provides excellent summary of prior methods in the palmprint literature and underlines state-of-art methods for online palmprint identification, which has also been focus of our work. Reference [28] is the first paper on the 3D palmprint identification published in 2008. In this paper, we present a general framework which can unify several state-of-art 2D and 3D palmprint identification methods.

The key contributions from this paper can be summarized as follows:

- We present a unified framework for the palmprint identification and use this framework to argue that (a) one-to-one matching strategy and (b) binary representation of features is more accurate and effective strategies for the palmprint identification. We also provide theoretical justification for the effectiveness of binary features to support the second argument. These two arguments are used to develop a new approach for 2D palmprint matching (referred as to *Fast* matching in this paper). Our experimental results on several publicly available contact-less and contact-based palmprint databases illustrate significantly improvement performance over other competing methods in the literature. Our experimental results also demonstrate other key advantages in addition to improving the matching accuracy, which lies in significantly reduced template size (66.7% at least), significantly reduced feature extraction time (66.7% at least) and the matching time (98.6% at most), making it most suitable palmprint matching approach to-date, especially for large scale and online applications.
- These two arguments are evaluated for the 3D palmprint matching and used to propose a new method of 3D palmprint feature extraction and matching. The proposed approach outperforms currently available 3D palmprint matchers in the literature. Our experimental results on public available contact-less and contact-based palmprint databases of 177 and 200 subjects not only significantly outperform the other 3D palmprint methods, but also significantly reduces the template size (66.7% at least),

Manuscript received October 5, 2014; revised December 1, 2014 and March 5, 2015; accepted April 11, 2015. Date of publication November 23, 2015; date of current version January 18, 2016. This work was supported by project grant no. A-SA79 under The Hong Kong Polytechnic University and Zhejiang University Joint Supervision scheme. The associate editor coordinating the review of this manuscript and approving it for publication was Prof. Zhenan Sun.

Q. Zheng is with the Department of Computing, The Hong Kong Polytechnic University, Hong Kong, and also with the Department of Computer Science and Technology, Zhejiang University, Hangzhou 310027, China (e-mail: zq20040233@zju.edu.cn).

A. Kumar is with the Department of Computing, The Hong Kong Polytechnic University, Hong Kong (e-mail: ajaykr@ieee.org).

G. Pan is with the Department of Computer Science and Technology, Zhejiang University, Hangzhou 310027, China (e-mail: gpan@zju.edu.cn).

Color versions of one or more of the figures in this paper are available online at http://ieeexplore.ieee.org.

Digital Object Identifier 10.1109/TIFS.2015.2503265

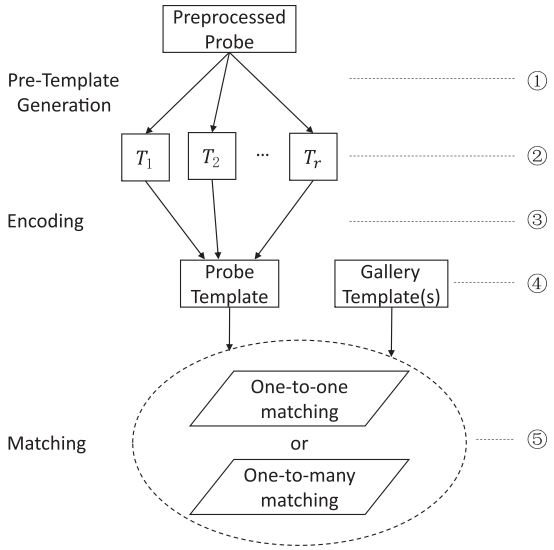

Fig. 1. A Unified Framework for Palmprint Identification.

feature extraction time (66.7% at least) and feature matching time (66.7% at least).

The rest of this paper is organized as follows. Section II introduces the unified framework for the palmprint identification. Comparison among several competing palmprint identification methods in the literature, two arguments as well as a theoretical analysis for the second argument are also presented in this section. In Section III, a novel 3D palmprint feature is proposed. The experimental results from five public available palmprint databases are reported in Section IV which describes key conlusion from this paper. Section V concludes this paper.

II. Palmprint Matching

In this section, we argue that *one-to-one* matching strategy and the binary feature representation is expected to be more accurate and efficient approach for the palmprint matching. We firstly introduce a general framework for the palmprint identification.

A. A Unified Framework for Palmprint Identification

In order to comparatively analyze most promising and competing palmprint identification methods in the literature, we firstly present a generalized framework. Assuming that all the palmprint images in the dataset are preprocessed, such as the image normalization and the region of interest segmentation, this framework is generalized to unify feature extraction and matching stage for the palmprint identification.

As shown in Figure 1, the feature extraction stage consists of pre-template generation followed by their consolidation in encoding stage. The $T_1, T_2 \ldots$ describe the intermediate results usually generated by the convolution operation between filters and the preprocessed probe. Encoding of these multiple intermediate results generates the final feature template which can effectively characterize the palmprint image. The encoding operation is usually some kind of voting technique, like max or min operation, *i.e.*, at certain position of the generalized feature. Supporting T_k represents the max value over other pre-templates, then k is marked as the feature of current position.

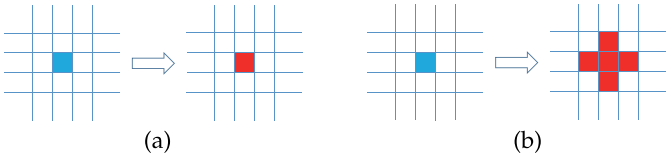

Fig. 2. (a) One-to-one and (b) one-to-many matching strategy.

The probe template, regarded as feature, is matched to templates generated from the gallery. Each template can be seen as a feature matrix, each entry on the matrix is an encoded feature code. The feature code is generated by voting scheme from several pre-templates. Distance between the two templates is defined as the sum of distance between such codes.

There are two kinds of prominent template/feature matching strategy successfully used in the literature, *i.e.* (a) *one-to-one* and (b) *one-to-many* matching strategy. For one-to-one matching strategy, the Hamming distance between the codes with same position is returned as the final distance. For one-to-many matching strategy, the code in one template matrix is matched to the neighborhood of the corresponding code in another matrix, and the minimum Hamming distance is returned as the final distance. Figure 2 illustrates these two strategies. Each block in this figure represents a feature code.

The Ordinal Code [18], robust line orientation code (RLOC) [7] and the competitive code (CompCode) [10] can be considered as most competing and state-of-art palmprint identification methods reported in the literature.[1] These methods are highly efficient and suitable for the online palmprint matching and therefore can be considered as competing. These methods are also summarized in Table I.

During the feature extraction stage, both of the CompCode and RLOC use six spatial filters to extract dominant texture orientation and generate one feature template. In the matching stage, they use one-to-one matching strategy and one-to-many matching strategy respectively. The feature extraction stage of the Ordinal Code only use two filters to extract feature and for each probe, the processing is repeated three times and therefore three feature templates are generated. In the matching stage, it employs one-to-one matching strategy and the sum of three distances is the final matching distance. Table I, which is corresponding to the framework in Figure 1, summarizes these three competing methods using pre-template generation, number of encoding classes for each code and matching strategy. For simplicity, the number of encoding classes for each code is represented by λ in the following analysis.

B. Motivation

There are two key challenges in accurately matching two palmprint images. The first one is relating to the accurate representation of features which is seriously influenced by

[1]The performance for palm code [20] or fusion code [14] approaches are far below as compared to these three methods.

TABLE I
SUMMARY OF SEVERAL COMPETING 2D PALMPRINT MATCHERS

Method	① Pre-template generation method	② Number of pre-template (r)	③ Encoding method	④ Number of encoding classes (λ)	⑤ Matching method
CompCode [10]	convolution	6	min	6	one-to-one
RLOC [7]	convolution	6	min	6	one-to-many
Ordinal Code [18]	convolution	2	max / min	2	one-to-one

the noise introduced on the surface due to sweat, dirt, etc. The other challenge is resulting from inaccurate alignment of matched palmprints which is mainly contributed from the palmprint deformations due to surface pressure such as stretching, as palm is not a rigid surface.

Most efficient methods reported in the literature employ feature encoding strategy instead of using the numerical feature values as the representative feature. Such discretization of precise feature values reduces the influence of noise and also helps to enhance matching speed [15]. The one-to-many matching strategy may help to accommodate the misalignment between the matched templates which is mainly introduced due to the deformations during the imaging [7].

According to the results reported in [7] and [18], the performance of RLOC and the Ordinal Code are superior to that of CompCode. The comparative analysis between these methods is discussed in the following and used to develop our two arguments. We also perform a series of experiments on publicly available databases and provide experimental results in Section IV, which further validate/support these two arguments.

1) RLOC VS CompCode: According to [7], the difference between RLOC and CompCode lies in feature extraction and matching stage. RLOC uses different filter to generate pre-templates and employs one-to-many matching stage. However, the matching speed from this strategy is very slow (the matching speed of the CompCode is nearly 25 times faster than that of RLOC). Besides, from our experimental results, we find one-to-many strategy even degrades the matching performance. Such degradation can be attributed due to two main reasons: 1) the deformation of palmprint data is not very significant; 2) because of the local continuity in feature codes and limiting encoding results, the influence of misalignment is reduced during the feature matching. Therefore, we can conclude that for contact palmprint data the misalignment cause by the surface deformation is not so serious and can be reduced by some appropriately encoding strategy. Our experimental result reported in Section IV also supports such analysis. Therefore, our first argument is that methods employing one-to-one matching strategy is to be more efficient and accurate for palmprint matching.

*2) Ordinal Code **VS** CompCode:* The encoding class number (λ) for the Ordinal Code is 2 while that of the CompCode is 6. The Ordinal Code achieves significant improvement over the CompCode. Note that for Ordinal Code, the feature extraction stage repeats three times. However, we find even performing the feature extraction once, the methods with $\lambda = 2$ are more effective as illustrated from our experiment results. Therefore, our second argument is that the features which are encoded using $\lambda = 2$ are more effective than those with $\lambda > 2$. Our theoretical analysis to further support our argument is detailed in the following section.

C. Analysis on Palmprint Matching

Previous work [7], [9], [10], [18], [20] used a feature matrix to represent the features from the palmprint image. The elements in such feature matrix is always an integer number which represents encoded feature or the feature code. The sum of code distances between all elements of feature matrix is used to compute the matrix distance between feature matrixes. Each entry of the feature matrix is binarized and the Hamming distance is employed to measure the codes' matching distance. For simplicity, we consider two codes' distance is *zero* if they are the same or have the same feature values, otherwise not.

When two palmprint templates from the same subject are being matched to ascertain their similarity, we call this similarity distance as intra-class matching distance or the genuine matching distance. When two such matched palmprints belong to two different subjects, the matching distance is referred to as inter-class matching distance or imposter matching distance.

Let us firstly characterize inter-class matching attempts between two palmprints which are here from two different subjects and are unknown. Such matching attempts are effectively random events as the likelihood of the codes, representing the palmprint features, can be matched or not matched is equal. Therefore we can reasonable assume[2] that the distribution of inter-class matching distance D_{inter} follows Binomial distribution and can be represented as follows:

$$D_{inter} \sim B(n_{inter}, p), \tag{1}$$

where p is the success probability, and n_{inter} represents the number or matching attempts or trials which also depends on the size of feature matrix. A well-designed feature extractor is expected to generate encoded code/results which have equally likely chance of being present in the feature template. Therefore the probability of each of the encoded results/code in the template should be $\frac{1}{\lambda}$. For inter-class matching, two feature matrixes are expected to be uncorrelated, therefore we can assume that

$$p = 1 - \frac{1}{\lambda}. \tag{2}$$

Two inter-class distance distributions with λ being 6 and 2 respectively are shown in Figure 3(a).[3]

We now analyze the intra-class matching attempts and characterize the matched code pairs as reliable if both of the

[2]Analysis of iris codes using millions of matching scores presented by Daugman [11] also justifies this assumption.

[3]For easy illustration, we assign n_{inter} a certain number 1000.

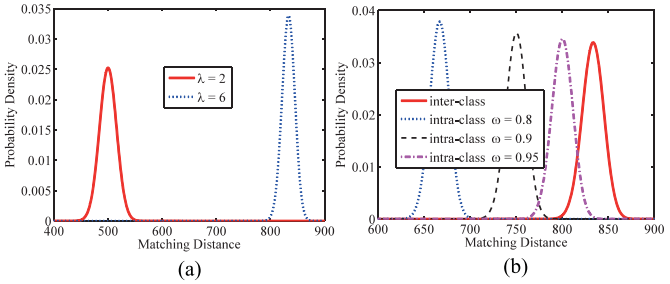

Fig. 3. (a) Typical matching distance distribution for different λ. (b) When $\lambda = 6$, the inter-class distance distribution and three intra-class distance distribution with different ω.

participating matching codes are encoded in the right class,[4] otherwise we call the codes pair unreliable. The matching distances between such reliable code pairs is expected to be certainly *zero*. However for the unreliable ones, their matching distances can still have chance to be *zero*. Therefore the number of unreliable code pairs will effectively determine the average intra-class matching distance. It may be noted that the unreliable codes are mainly generated due to the influence of imaging noise and/or image misalignment, and the impact of such influences is unknown. Therefore whether these unreliable codes can be matched or not matched can be considered as random (equally likely) event. Similarly we assume intra-class matching distance D_{intra} follows the Binomial distribution

$$D_{intra} \sim B(n_{intra}, p), \tag{3}$$

n_{intra} is the unreliable pairs number which should be smaller than the total number of matching code pairs. Representing $\omega (0 < \omega < 1)$ as the unreliable pairs rate, on the same database and for a given feature extractor, we have same size for the matching templates, thus we get $n_{intra} = \omega n_{inter}$. p is the success possibility. For the unreliable pairs, as analysis above, it is quite similar as that of inter-class matching pair. Thus, we assume it is the same as in inter-class matching distribution as defined in Equation 2.

Figure 3 (b) illustrates a typical distribution of inter-class and intra-class matching scores with different ω. It can be observed that when ω becomes larger, the overlapping area between inter- and intra-class distributions also becomes larger which can significantly degrade the palmprint matching performance. In order to achieve accurate matching performance, least overlap between two distributions is desirable which can be achieved with the smaller value of ω.

Given a p, the likelihood θ that an unreliable pair is successfully matched can be estimated as follows

$$\theta = 1 - (1 - p)(1 - p). \tag{4}$$

Note that ω represents the unreliable code pairs amount, we make a reasonable assumption that ω is proportional to θ, *i.e.*

$$\omega \propto \theta. \tag{5}$$

[4]Right class describes the actual texture/depth information.

Combining Equation (2) and Equation (4), Equation (5) can be rewritten as

$$\omega \propto 1 - \frac{1}{\lambda^2}. \tag{6}$$

From Equation (6) we can observe that the smaller λ resulting in the smaller ω. Therefore, $\lambda = 2$ is desirable number of classes for encoding the extracted features.

The analysis above argues the effectiveness of binary feature representation for the palmprint. This argument is further supported by our experimental results on 2D palmprint database reported in Section IV.

III. 3D Palmprint Identification

There has been very little attention on the development of algorithms for the accurate 3D palmprint matching. In this section, we provide a brief introduction to currently used 3D palmprint features and unify these features into our proposed palmprint framework (Figure 1). This framework is then used to develop a novel feature representation for more accurately and efficiently matching 3D palmprint images.

A. 3D Feature for Palmprint

We can classify 3D palmprint features investigated in the literature into two categories. The first one is based on the SI (shape index) [12]. The SI has been widely employed to detect the feature point on 3D face surface [13], [17], [19]. Kanhangad *et al.* [1], [2] introduced this approach for the 3D palmprint surface matching and developed the surface code. They firstly estimated the curvature from the depth image. The surface code is the classification result according to the SI feature. The matching strategy employed by this method is essentially one-to-one matching.

Another 3D palmprint feature has been explored by Li *et al.* [8], [16] which is named as the orientation-feature. They firstly preprocessed the depth image to generate MCI (mean curvature image). Then the feature extraction method, similar to the CompCode, is employed on the MCI to extract the orientation-feature. Their matching strategy is also one-to-one strategy. In their paper, fused matching score between line-feature and orientation-feature is used for the final matching. In our analysis and experiment, only the orientation-feature is used for the fair comparison mainly for three reasons: 1) The performance using only line-feature is very poor; 2) similar fusion strategy can be applied between line-feature and surface code or our feature; 3) line-feature is quite different from orientation-feature, surface code and our feature proposed in this paper.

These two methods can also be unified in our general palmprint identification framework. For surface code, one intermediate pre-template related to curvature is firstly generated. The classification strategy is applied on the intermediate result to generate the final feature code. Orientation-feature is exactly same as the CompCode which introduce in previous section. One-to-one matching strategy is employed on both of these methods. Table II presents key parameters and feature of these two methods using framework shown in Figure 1.

TABLE II
SUMMARY OF 3D PALMPRINT MATCHERS

Method	① Pre-template generation method	② Number of pre-template (r)	③ Encoding method	④ Number of encoding classes (λ)	⑤ Matching method
Surface code [2]	curvature calculation	1	classification	9	one-to-one
Orientation-feature [8]	convolution	6	min	6	one-to-one
Ours	convolution	2	max / min	2	one-to-one

B. Binary Feature Representation for 3D Palmprint

It can be observed from Table II that the λ for currently developed 3D palmprint methods is larger than 2. According to above analysis, the feature with λ being 2 is expected to achieve superior performance. Therefore, we propose a simple feature for 3D palmprint matching based on above analysis. Before introducing our feature, we firstly define a spatial filter.

Given a filter $f(n)$ with size $n \times n$, all the entries of $f_{i,j}(n), i, j \in [1, n]$ are set to be $\frac{1}{n^2}$. In the pre-template generation stage, our method performs convolution operation between the acquired depth image and these two filters separately and two intermediate pre-templates are generated. Maximum/Minimum encoding method is applied on the two intermediate results to generate the feature. More specifically, the binary feature matrix F is computed as follows

$$F_{i,j} = \tau([f(n) * I - f(m) * I]_{i,j}), \tag{7}$$

where $F_{i,j}$ is the feature value at position (i, j), I is the preprocessed image, $*$ is convolution operation, n and m are given parameters, $[O]_{i,j}$ is the value of matrix O at position (i, j), $\tau(\cdot)$ is defined as

$$\tau(\alpha) = \begin{cases} 0, & \alpha < 0 \\ 1, & \alpha \geq 0. \end{cases} \tag{8}$$

Two matrixes, $f(n) * I$ and $f(m) * I$, are two intermediate pre-templates (Figure 1). The substraction operation is equivalent to max, min operation as step 3 in the framework. The parameters of the proposed feature in our framework are shown in Table II. By simple derivation of Equation 7, we can efficiently use one filter $g(n, m)$ instead of $f(n)$, $f(m)$ and the feature extraction equation can be rewritten as

$$F_{i,j} = \tau([g(n, m) * I]_{i,j}). \tag{9}$$

The value of $g(n, m)$ at position (i, j) is defined as

$$g_{i,j}(n, m) = \begin{cases} m^2 - n^2, & |i - \frac{m}{2}| < \frac{n}{2} \ \& \ |j - \frac{m}{2}| < \frac{n}{2} \\ -n^2, & otherwise, \end{cases} \quad i, j \in [1, m], m > n. \tag{10}$$

The shape of $g(n, m)$ is similar to a hat (see Figure 4). Each code resulting from spatial filtering operation describes the shape of corresponding point on the 3D palmprint images, which is either convex or concave.

C. Matching

The one-to-one feature matching strategy is incorporated for our method. Since the feature is binary representation, the Hamming distance is equivalent to *XOR* distance. The matching distance between two feature matrix A and B can be computed as follows:

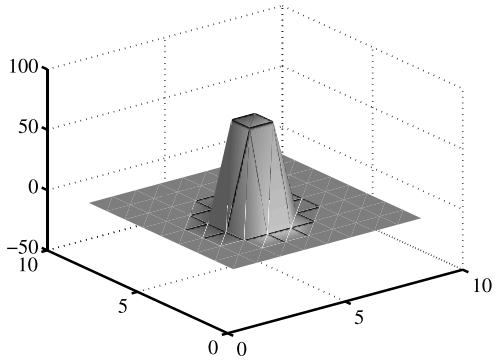

Fig. 4. Spatial representation of a typical 2D filter $g(3, 9)$.

$$Dis(A, B) = \frac{\Gamma(A \otimes B \& M(A) \& M(B))}{\Gamma(M(A) \& M(B))}, \tag{11}$$

$\otimes$ and & are logical XOR and AND operation, $\Gamma(A)$ computes the number of non-zero value in matrix A, $M(\cdot)$ is the mask matrix indicating the valid region on palmprint image which is define as

$$M_{i,j}(P) = \begin{cases} 0, & I_{i,j}(P) > \alpha \\ 1, & otherwise, \end{cases} \tag{12}$$

$I_{i,j}(P)$ is the value of depth image P at position (i, j), α is a given parameter that describes the distance which is far away from the acquisition sensor.

IV. EXPERIMENTAL RESULTS

We present experimental results from three publicly available 2D palmprint and 3D palmprint databases. The verification experiments on 2D palmprint are used to evaluate two arguments presented in Section II-C: 1) methods employing one-to-one matching strategy is more efficient than those employing one-to-many matching strategy and 2) binary representation for the feature is more accurate and efficient, *i.e.* the methods with $\lambda = 2$ is more accurate and efficient than methods with $\lambda = 6$.

We use two publicly available 3D palmprint databases to evaluate the effectiveness of the proposed 3D palmprint feature. There are few 3D palmprint matching methods available in the literature. Therefore the experimental comparisons are performed with the features proposed by the respective papers which introduced these databases in the public domain.

TABLE III

THE COMPARISON OF DIFFERENT METHODS ON POLYU PALMPRINT DATABASE

Method	Fast-RLOC	RLOC (in [7])	RLOC	Fast-CompCode	CompCode (in [7])	CompCode
FAR (%)	4×10^{-5}	4×10^{-5}	4×10^{-5}	4×10^{-5}	4×10^{-5}	4×10^{-5}
FRR (%)	**0.94**	1.631	2.10	**0.31**	4.86	2.90
EER (%)	**0.089**	0.16	0.30	**0.041**	0.47	0.76

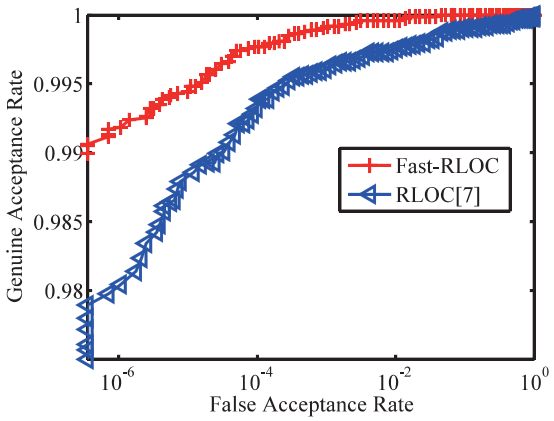

Fig. 5. The ROC curves for Fast-RLOC and RLOC.

A. 2D Palmprint: Experiment I

In order to validate the first argument, we modify the matching stage of RLOC from one-to-many strategy to one-to-one matching strategy. The feature extraction stage remains unchanged. We refer the modified one as Fast-RLOC. In [7], where the RLOC is proposed, PolyU palmprint database [4] is used to establish superiority of RLOC than other methods. In order to make our argument more persuasive, the same database with same protocol is employed in this experiment.

The PolyU palmprint database contains 7,752 palmprint images with 193 individuals which is divided into 386 classes. The provided images are cropped to the size of 128×128. As reported in [7], only the first sample of each individual is used to construct the training set. The training set is enlarged by rotating each image in training set at 9°, 6°, 3°, −3°, −6° and −9° respectively. Consequently, there are totally seven training samples for each subject. All the remaining images are used for testing and there are 7,366 probes.

The ROC curve is shown in Figure 5. Table III shows the comparison for Fast-RLOC and RLOC (our implementation [3] as well as the author's results reported in [7]). From the curves and table, the performance achieved by Fast-RLOC is significantly superior to the best result reported in [7].

Besides, the computation time for the matching of Fast-RLOC is significantly smaller, *i.e.* about 70 times faster than that of RLOC (Table IV). From the result, we can draw the conclusion that for palmprint matching, the method employing one-to-one matching strategy not only achieves superior matching accuracy but also significantly reduces the computation time.

B. 2D Palmprint: Experiment II

The experiments in this section are used to verify the argument on the effectiveness of binary feature representation for 2D palmprint matching. Firstly, we simplify the CompCode to generate binary representation for feature. As analyzed in Section II-B, the CompCode uses six filters to generate six pre-templates. In the simplified version, two of the six filters (the orientation of these two filters are orthogonal) are used to generate two intermediate pre-templates and consequently binary template is generated as final feature. The rest of implementation of the CompCode remains unchanged. In this paper, we refer this method as Fast-CompCode.

TABLE IV

THE MATCHING SPEED (*ms*) COMPARISON BETWEEN FAST-RLOC AND RLOC

Method	Matching
Fast-RLOC	**0.017**
RLOC	1.2

Note: The experimental environment for all the experiments in this paper is: Windows 8 Professional, Intel(R) Core(TM) i5-3210M CPU@2.50GHz, 8G RAM, VS 2010

The experiments are performed on the same database with same protocol as above (the same as in [7]). This experimental setting is primarily for two reasons:

- The CompCode and RLOC are introduced in [10] and [7] respectively and evaluated on the same PolyU 2D palmprint database [4]. Considering the performance of RLOC is superior to the CompCode as reported in [7], the protocol in [7] is more challenging.
- Considering the publication sequence and research group of the CompCode [10] and RLOC [7]. The CompCode result in [7] is excepted to be reliable for our comparison.

Figure 6 (c) shows the ROC curves for Fast-CompCode and the CompCode in for experiment. As can be observed from the results, the performance of simplified one is superior to that of original one. In order to make the comparison more reliable and fair, in addition to our implementation [3], the results reported in [7] are also shown in Table III.

We also perform the Fast-CompCode method on other three publicly available 2D palmprint databases: PolyU contactless 2D/3D palmprint database [5], IITD database [22] and CASIA palmprint database [23]. Different protocols reported in [2], [25], and [26] are applied on these three databases respectively for fair comparison. The ROC curves are shown in Figure 6.

As can be observed from Figure 6 and Table III, the Fast-CompCode achieves the better performance. Table V shows that the feature extraction and matching time of binary feature representation is significantly smaller and its template size is also significantly smaller. Therefore we can conclude that binary feature representation is not only more accurate but also significantly more efficient.

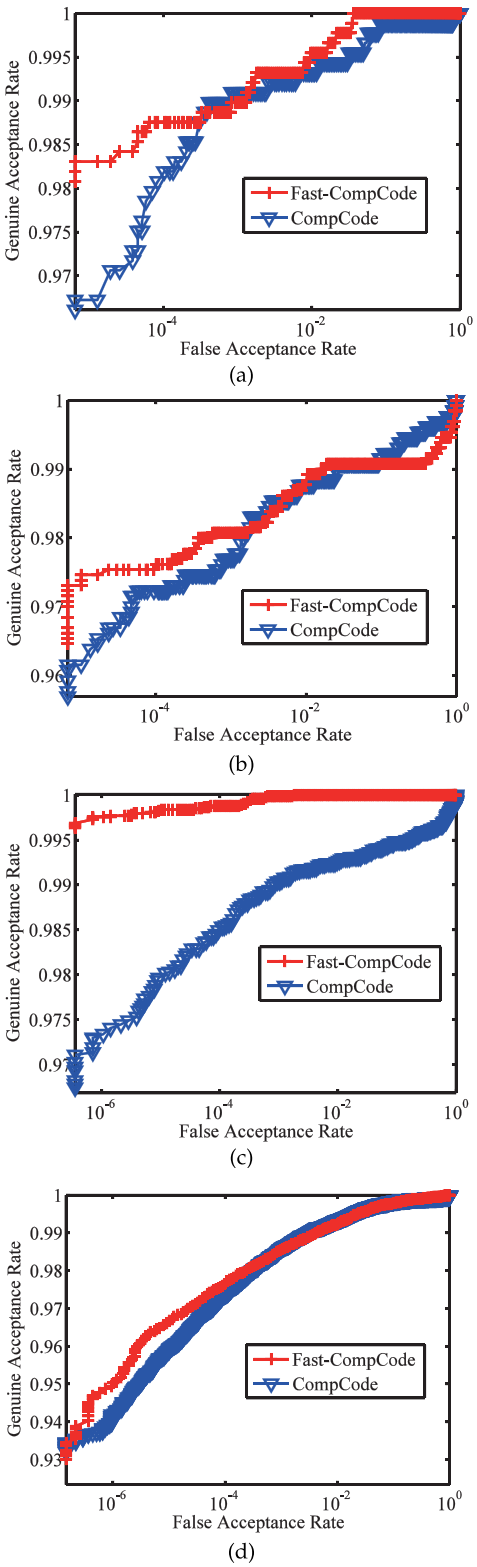

Fig. 6. The ROC curves for Fast-CompCode and CompCode on (a) PolyU contactless 2D/3D palmprint database, (b) IITD, (c) PolyU palmprint database and (d) CASIA palmprint database.

C. 3D Palmprint: Experiment I

The first 3D palmprint database used for evaluation is PolyU contactless 2D/3D palmprint database [5]. There are 177 palms collected in two sessions, each palms has 10 2D images and 10 depth images. It also provides segmented palmprint images and the size of each segmented image is 128 × 128. Our experiments are performed on the 3D part of this database. For each palmprint, we use the first 5 samples to construct the training set and the remained 5 samples as testing samples, totally 885 for training and 885 as testing samples. The surface code used for palmprint matching proposed in [1] and [2] is used for comparison.

TABLE V

THE TEMPLATE SIZE (*bytes*), FEATURE EXTRACTION (FEAEXT) TIME (*ms*) AND MATCHING TIME (*ms*) COMPARISON BETWEEN FAST-COMPCODE AND COMPCODE

Method	Template Size	FeaExt	Matching
Fast-CompCode	**128**	**1.3**	**0.017**
CompCode	384	4.0	0.054

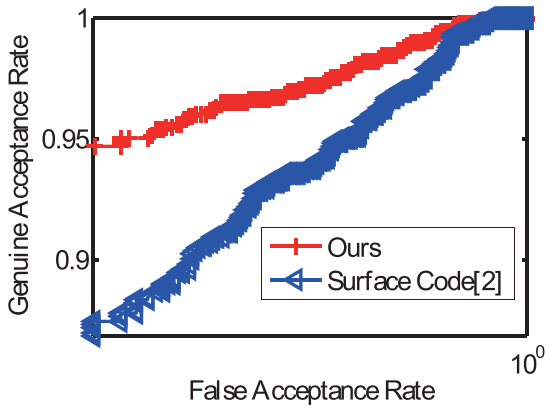

Fig. 7. The ROC curves for surface code and our method.

TABLE VI

THE TEMPLATE SIZE (*bytes*), FEATURE EXTRACTION (FEAEXT) TIME (*ms*) AND MATCHING TIME (*ms*) COMPARISON AMONG OUR METHOD, SURFACE CODE AND ORIENTATION-FEATURE

Method	Template Size	FeaExt	Matching
Ours	**128**	**1.3**	**0.017**
Surface code	512	53.3	0.072
Orientation	384	4.0	0.054

The ROC curve is used to evaluate the matching performance (Figure 7). The EER from our method is 1.84% while the EER from surface code is 3.20%. The template size, feature extraction speed and matching speed comparison is shown in Table VI. The performance from our method is significantly superior to that from surface code. Besides, the template size and computational cost of our method is significantly smaller.

D. 3D Palmprint: Experiment II

The PolyU 2D_3D palmprint database [6] is the second 3D palmprint database to evaluate the proposed method. It is a contact-based palmprint database from 200 subjects and has 8000 samples. The left and right palmprints from same person can be considered as belonging to different classes, and the total class number is 400. There are two sessions for each class. For each class in each session, the sample number is 10. This database also provides segmented palmprint images, and the size of ROI is 128 × 128.

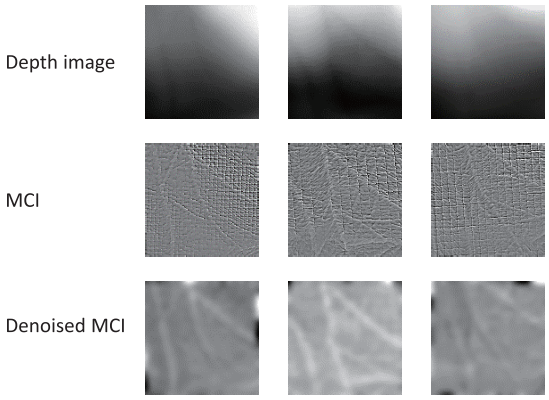

Fig. 8. Three 3D palmprint images, their corresponding MCI, and denoised MCI.

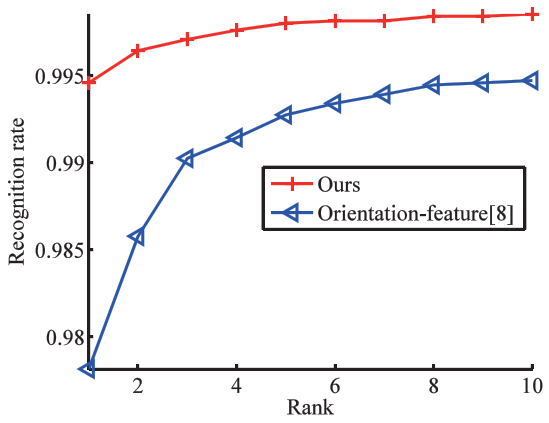

Fig. 9. The CMC curves for our method and orientation-feature.

The 3D part of this database is quite noisy as also mentioned in reference [8]. It is a kind of high-frequency noise and is mainly caused by the electrical circuit hardware used for structured light based imaging. Therefore, our experiments are performed on the preprocessed 3D depth image just like as done in [8]. The preprocessing method consists of MCI (mean curvature image) generation and denoising operation. Figure 8 shows the visualization of several samples.

In order to compare the orientation-feature proposed in [8], two experiments for this database are performed, one for verification and the other for recognition, just the same as in [8].

1) Recognition: In the recognition experiment, the first sample of each class in the database is used to construct the training set and the other samples are used as probes. Therefore, there are 7,600 probes and 400 training samples. The CMC curves of our method and orientation-feature are shown in Figure 9. As can be observed, our method outperforms the orientation-feature based the methods in [8].

2) Verification: In the verification experiment, each sample is matched to the other samples to generate genuine or imposter score. There are 76,000 genuine matching scores and 31,920,000 imposter matching scores. The ROC curves of our method and orientation-feature are shown in Figure 10. The EER from our method is 0.48% while that from

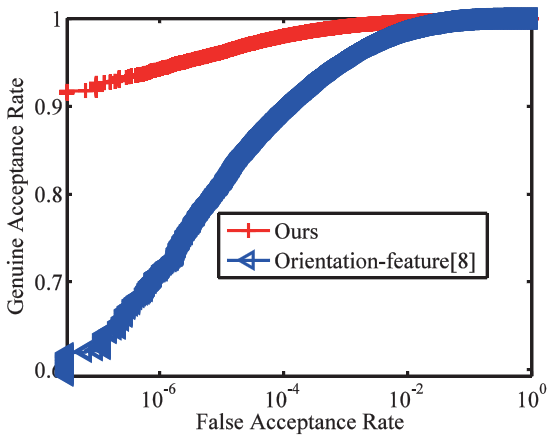

Fig. 10. The ROC curves for our method and orientation-feature.

orientation-feature is 1.12%. The comparison between our method and orientation-feature in Table VI and Figure 10 again confirms that the proposed method is significantly more accurate, efficient and results in smaller template size.

V. Conclusions and Future Work

The paper presented a general framework for 2D and 3D palmprint recognition. Several state-of-art 2D and 3D palmprint identification methods can be unified into this framework. This framework is used to introduce two arguments for palmprint matching. We presented statistical model analysis and the experimental results on severval publicly available 2D palmprint databases have been employed to support these two arguments. Our proposed methods not only achieves superior performance but also results in significantly reduced template size, the feature extraction time and the matching time. We also validated these two arguments for the 3D palmprint database and use them to develop a novel 3D palmprint feature representation. Our experimental results on two publicly available contactless and contact-based databases suggest the proposed method is significantly more faster, more accurate and results in the least template size. Reference [29] is more recent work on 3D palmprint which almost concurrently is made available but after the submission of this manuscript. However it is not difficult to observe that our method of 3D palmprint identification is more accurate (CMC in Fig. 9 and rank-one accuracy from [29, Tables 3 and 4]) and also significantly faster which is primarily due to the simplicity of the feature extractor. The method detailed in [29] is quite promising and essentially combines 3D palmprint surface codes in [2] with the methods in the literature [30], [31]. It is surprising that reference [29] does not provide any ROC or CMC, only uses one of the publicly available databases, and therefore raises many questions on the performance evaluation.

Despite the outperforming results and significant advancement to the state-of-the-art in palmprint identification, there are several open issues which need to be addressed in future work. Our work in this paper only considered single scale analysis. However the multi-scale analysis, as in [26] is expected to further improve the performance and is part of our future work. Further work is also required to develop theoretical proof for

the first argument as it is not yet fully addressed in this work. Identification of palmprint images acquired from wild and at-a-distance can help to enhance the applicability of palmprint matching in new domains and is part of our on-going part of our further work.

REFERENCES

[1] V. Kanhangad, A. Kumar, and D. Zhang, "Contactless and pose invariant biometric identification using hand surface," *IEEE Trans. Image Process.*, vol. 6, no. 3, pp. 1415–1424, May 2011.

[2] V. Kanhangad, A. Kumar, and D. Zhang, "A unified framework for contactless hand verification," *IEEE Trans. Inf. Forensics Security*, vol. 20, no. 5, pp. 1415–1424, May 2011.

[3] The Hong Kong Polytechnic University. (2015). *Implementation Codes for 3D Palmprint Matching*. [online]. Available: http://www.comp.polyu.edu.hk/~csajaykr/3DPalmprint.htm

[4] (2013). *PolyU Palmprint Database*. [Online]. Available: http://www.comp.polyu.edu.hk/~biometrics

[5] (2013). *The Hong Kong Polytechnic University Contact-Free 3D/2D Hand Images Database (Ver 1.0)*. [Online]. Available: http://www.comp.polyu.edu.hk/~csajaykr/myhome/database_request/3dhand/Hand3D.htm

[6] (2014). *The Hong Kong Polytechnic University (PolyU) 2D 3D Palmprint Database*. [Online]. Available: http://www.comp.polyu.edu.hk/~biometrics/2D_3D_Palmprint.htm

[7] W. Jia, D.-S. Huang, and D. Zhang, "Palmprint verification based on robust line orientation code," *Pattern Recognit.*, vol. 31, no. 5, pp. 1504–1513, May 2008.

[8] W. Li, D. Zhang, L. Zhang, G. Lu, and J. Yan, "3-D palmprint recognition with joint line and orientation features," *IEEE Trans. Syst., Man, Cybern. C, Appl. Rev.*, vol. 41, no. 2, pp. 274–279, Mar. 2011.

[9] A. K. Jain and J. Feng, "Latent palmprint matching," *IEEE Trans. Pattern Anal. Mach. Intell.*, vol. 31, no. 6, pp. 1032–1047, Jun. 2009.

[10] A. W.-K. Kong and D. Zhang, "Competitive coding scheme for palmprint verification," in *Proc. 17th ICPR*, Washington, DC, USA, Aug. 2004, pp. 520–523.

[11] J. Daugman, "The importance of being random: Statistical principles of iris recognition," *Pattern Recognit.*, vol. 36, no. 2, pp. 279–297, 2003.

[12] C. Dorai and A. K. Jain, "COSMOS—A representation scheme for 3D free-form objects," *IEEE Trans. Pattern Anal. Mach. Intell.*, vol. 19, no. 10, pp. 1115–1130, Oct. 1997.

[13] T. C. Faltemier, K. W. Bowyer, and P. J. Flynn, "A region ensemble for 3-D face recognition," *IEEE Trans. Inf. Forensics Security*, vol. 3, no. 1, pp. 62–73, Mar. 2008.

[14] A. Kong, D. Zhang, and M. Kamel, "Palmprint identification using feature-level fusion," *Pattern Recognit.*, vol. 39, no. 3, pp. 478–487, Mar. 2006.

[15] A. Kumar and D. Zhang, "Hand-geometry recognition using entropy-based discretization," *IEEE Trans. Inf. Forensics Security*, vol. 2, no. 2, pp. 181–187, Jun. 2007.

[16] W. Li, L. Zhang, and D. Zhang, "Three dimensional palmprint recognition," in *Proc. IEEE Int. Conf. Syst., Man Cybern.*, Oct. 2009, pp. 4847–4852.

[17] X. Lu, D. Colbry, and A. K. Jain, "Three-dimensional model based face recognition," in *Proc. 17th Int. Conf. Pattern Recognit.*, Aug. 2004, pp. 362–366.

[18] Z. Sun, T. Tan, Y. Wang, and S. Z. Li, "Ordinal palmprint represention for personal identification [represention read representation]," in *Proc. IEEE Comput. Soc. Conf. Comput. Vis. Pattern Recognit.*, vol. 1. Jun. 2005, pp. 279–284.

[19] Y. Wang, G. Pan, Z. Wu, and S. Han, "Sphere-spin-image: A viewpoint-invariant surface representation for 3D face recognition," in *Proc. Int. Conf. 4th ICCS*, Kraków, Poland, Jun. 2004, pp. 427–434.

[20] D. Zhang, W.-K. Kong, J. You, and M. Wong, "Online palmprint identification," *IEEE Trans. Pattern Anal. Mach. Intell.*, vol. 25, no. 9, pp. 1041–1050, Sep. 2003.

[21] UIDAI. (2013). *Unique Identification Authority of India*. [Online]. Available: http://uidai.gov.in

[22] (Jan. 2014). *IIT Delhi Touchless Palmprint Database (Version 1.0)*. [Online]. Available: http://www.comp.polyu.edu.hk/~csajaykr/IITD/Database_Palm.htm

[23] (2013). *CASIA Palmprint Database*. [Online]. Available: http://www.cbsr.ia.ac.cn/PalmDatabase.htm

[24] (Mar. 2014). *HANIS, Home Affairs National Identification System, South Africa*. [Online]. Available: http://www.services.gov.za/services/content/news/verifyidentityonline/en_ZA

[25] A. Kumar, "Incorporating cohort information for reliable palmprint authentication," in *Proc. ICVGIP*, Dec. 2008, pp. 583–590.

[26] W. Zuo, Z. Lin, Z. Guo, and D. Zhang, "The multiscale competitive code via sparse representation for palmprint verification," in *Proc. IEEE Conf. Comput. Vis. Pattern Recognit.*, Jun. 2010, pp. 2265–2272.

[27] D. Zhang, W. Zuo, and F. Yue, "A comparative study of palmprint recognition algorithms," *ACM Comput. Surv.*, vol. 44, no. 1, Jan. 2012, Art. ID 2.

[28] V. Kanhangad, D. Zhang, and N. Luo, "A multimodal biometric authentication system based on 2D and 3D palmprint features," *Proc. SPIE*, vol. 6944, pp. 69440C-1–69440C-9, Mar. 2008.

[29] L. Zhang, Y. Shen, H. Li, and J. Lu, "3D palmprint identification using block-wise features and collaborative representation," *IEEE Trans. Pattern Anal. Mach. Intell.*, vol. 37, no. 8, pp. 1730–1736, Aug. 2015.

[30] A. Kumar, T.-S. Chan, and C.-W. Tan, "Human identification from at-a-distance face images using sparse representation of local iris features," in *Proc. ICB*, New Delhi, India, Mar./Apr. 2012, pp. 303–309.

[31] A. Kumar and T.-S. T. Chan, "Robust ear identification using sparse representation of local texture descriptors," *Pattern Recognit.*, vol. 46, no. 1, pp. 73–85, Jan. 2013.

Qian Zheng received the B.S. degree from the College of Computer Science and Technology, Zhejiang University, China, in 2011, where he is currently pursuing the Ph.D. degree with the College of Computer Science and Technology. He visited The Hong Kong Polytechnic University from 2013 to 2014 under a PolyU and Zhejiang University joint supervision scheme. He is currently a Research Assistant with The Hong Kong Polytechnic University. His current research interests include machine learning and computer vision.

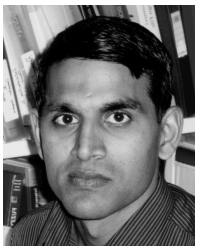

Ajay Kumar received the Ph.D. degree from The University of Hong Kong, Hong Kong, in 2001. He was an Assistant Professor with the Department of Electrical Engineering, IIT Delhi, Delhi, India, from 2005 to 2007. He is currently an Associate Professor with the Department of Computing, The Hong Kong Polytechnic University. He holds five U.S. patents, and has authored biometrics and computer vision-based industrial inspection. His current research interests are on biometrics with an emphasis on hand biometrics, vascular biometrics, iris, and multimodal biometrics. He is currently on the Editorial Board of *Pattern Recognition* journal and serves on the IEEE Biometrics Council as the Vice President (publications). He was on the Editorial Board of the IEEE TRANSACTIONS ON INFORMATION FORENSICS AND SECURITY from 2010 to 2013, and served on the Program Committees of several international conferences and workshops in the field of his research interest. He was the Program Chair for ICEB 2010 (Hong Kong) and Program Co-Chair for IJCB 2011 (Washington, DC), ICB 2013 (Madrid), and CVPR 2013, 2014, 2015 Biometrics Workshops. He has also served as the General Co-Chair of IJCB 2014 (Tampa) and ISBA 2015 (Hong Kong) and delivered the first tutorial on contactless 3D fingerprint identification during the CVPR 2015 held in Boston, USA.

Gang Pan received the B.Sc. and Ph.D. degrees in computer science from Zhejiang University, Hangzhou, China, in 1998 and 2004, respectively. He visited the University of California, Los Angeles, CA, USA, from 2007 to 2008. He is currently a Professor with the College of Computer Science and Technology, Zhejiang University. He has authored over 90 refereed papers. His current research interests include pervasive computing, computer vision, and pattern recognition. He has served as a program committee member for more than ten prestigious international conferences, such as ICCV and CVPR.